

Phys. C: Solid State Phys. 5, 2027 (1972).

⁴A. H. Cooke, S. J. Swithenby, and M. R. Wells, Solid State Commun. 10, 265 (1972).

⁵R. T. Harley, W. Hayes, and S. R. P. Smith, J. Phys. C: Solid State Phys. 5, 1501 (1972).

⁶R. L. Melcher, E. Pytte, and B. A. Scott, Phys. Rev. Lett. 31, 307 (1973).

⁷R. J. Birgeneau, L. G. van Uitert, J. K. Kjems, and G. Shirane, Phys. Rev. 10, 2512 (1974).

⁸P. -A. Lindgård, private communication.

Chemisorption Bond Length and Binding Location of Oxygen in a $p(2 \times 1)$ Overlayer on W(110) Using a Convergent, Perturbative, Low-Energy-Electron-Diffraction Calculation*

M. A. Van Hove and S. Y. Tong

Department of Physics and Surface Studies Laboratory, University of Wisconsin, Milwaukee, Milwaukee, Wisconsin 53201

(Received 23 June 1975)

A convergent perturbation scheme known as the layer-doubling method is used to determine the chemisorption position and bond length of an oxygen $p(2 \times 1)$ overlayer on W(110) surface. The use of perturbation treatment allows accurate and economical determination of surface crystallography on this strong-scattering material. Using eight phase shifts and 89 beams in the calculation, the oxygen atoms are found to occupy threefold-coordinated binding sites with a bond length of 2.08 Å.

The transition metal tungsten is probably the material most used as a substrate for chemisorption of gas atoms and molecules on its different crystal planes. Studies of surface properties of clean tungsten and the chemisorption of various gases on its surfaces have been carried out for many years using different surface-sensitive techniques. However, partly because of the very large atomic weight of the tungsten atom, there has been no accurate surface-structure determination of adsorbed atoms on any of the tungsten surfaces. We report here the first successful determination of surface structure of chemisorbed atoms on a tungsten surface. The binding location and chemisorption bond length of the $p(2 \times 1)$ oxygen overlayer on W(110) surface are determined using a convergent perturbation calculation¹ of the dynamical low-energy-electron-diffraction (LEED) approach. Our results here also differ from previous surface structures of overlayers determined on other metal substrates² in the following way. In all previous studies, the adsorbed foreign atoms settle at those surface sites that an atom of that substrate material would adsorb at, i.e., the bulk structure of the substrate extends into the overlayer. However, in the present case we find evidence to suggest that the oxygen atoms adsorbed on the W(110) surface do not reproduce the bulk structure of the substrate, but rather choose a site of higher coordination number to the substrate (a threefold-coordinated site).

The structures of clean W(100) and W(110) are

first determined.³ Our results show that for W(100) there is a possible contraction of about 6% of the topmost tungsten layer. On the W(110) surface, we find no contraction, expansion, or lateral shift of the topmost tungsten layer. Details of the surface structures on clean W(100) and W(110) are presented elsewhere.³ Recently Lagally, Buchholz, and Wang⁴ have used the constant-momentum-transfer averaging scheme on W(110) and come to the same conclusion that the (110) surface does not deviate from the bulk structure. In their averaging method, they concentrated on incident electron energies above 150 eV, because below 150 eV the averaging scheme is much more difficult to use. Since our dynamical analyses are primarily done at energies below 200 eV (15 to 200 eV), the agreement between our results and those of Ref. 4 on the surface structure of clean W(110) is significant as it demonstrates the consistency of the two methods using experimental data with almost mutually exclusive energy ranges.

For the $p(2 \times 1)$ oxygen overlayer on W(110), a number of surface structures have previously been suggested. However, the results of Lagally, Buchholz, and Wang⁴ showed that, contrary to previous speculations, there is no reconstruction of the tungsten atoms by the oxygen overlayer. Because they worked at energies above 150 eV, the averaging technique cannot tell the position of the oxygen atom. For a simple $p(2 \times 1)$ oxygen overlayer on W(110), we show in Fig. 1

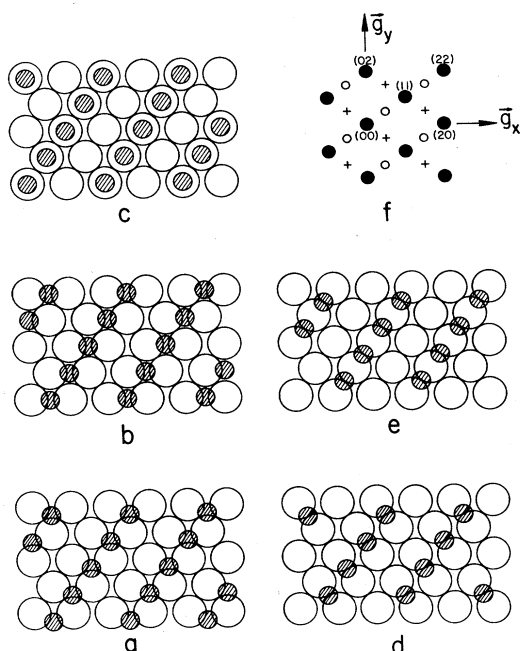


FIG. 1. Possible chemisorption sites of the $W(110) + p(2 \times 1)O$ surface. Large circles denote tungsten atoms, small circles denote overlayer atoms. (a) Adsorption in the threefold sites, (b) center sites, (c) peak sites, (d) and (e) two nonequivalent bridge sites. All the geometries shown produce the diffraction pattern in (f), with the half-order spots denoted +; an overlayer domain mirrored in the x - z plane would produce the half-order spots denoted O.

the different likely adsorption sites that an oxygen atom may occupy. The "center" site (b) is the bulklike position that a tungsten atom would occupy if another tungsten layer were added. The threefold site (a) is the position we suggest for the oxygen adsorption. At this location, the oxygen atom sits equidistantly above three tungsten atoms, so it has three nearest neighbors, compared to only two nearest neighbors at the center location. Figure 1(c) shows the "peak" site and (d) and (e) show the "bridge" sites. The two bridge sites differ in that bridges can be directed crosswise to the one-dimensional rows of oxygen atoms that characterize the overlayer [shown in (d)], or they can be directed parallel to these rows [shown in (e)]. In the threefold site, the $p(2 \times 1)$ oxygen overlayer has no two-dimensional symmetry (mirrors or axes), whereas all the other sites have twofold rotational symmetry axes.

In the calculation for the LEED intensity-energy (I - V) spectra, the layer-doubling method is

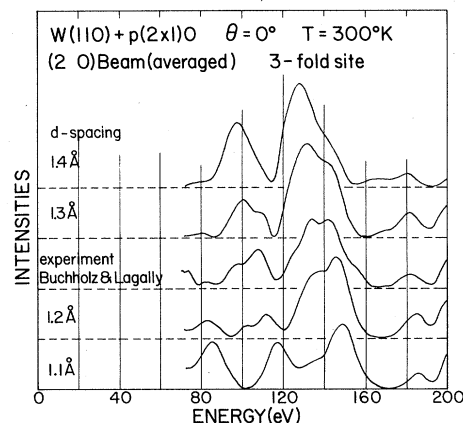


FIG. 2. Experimental (middle curve) and calculated I - V curves for the (20) beam (averaged over domains) diffracted from the $W(110) + p(2 \times 1)O$ surface. The calculated curves apply to the threefold site with interlayer spacings 1.1 to 1.4 Å. The experimental curve is taken from Ref. 7

used. This is a convergent interaction method which is accurate and fast. Eight phase shifts are used for both the oxygen overlayer and the tungsten substrate, and a maximum of 89 beams are included. At each energy, the number of iterations and number of beams are carefully chosen to ensure proper numerical convergence. For the tungsten substrate, two superposition potentials are tested⁵ and they are found to give very similar calculated I - V curves. For the oxygen overlayer, a superposition potential obtained by overlapping atomic charge densities is employed.⁶ A constant inelastic damping of 5 eV and an inner potential of 10 eV are used. These

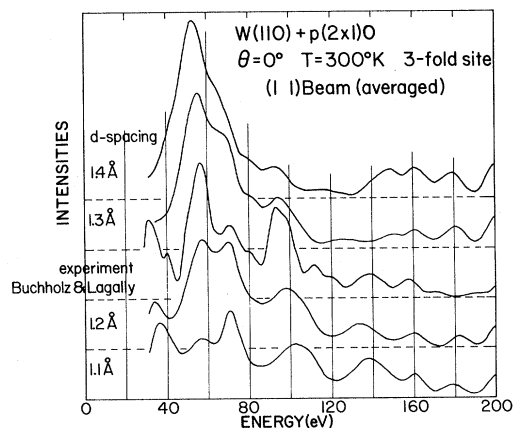


FIG. 3. The same as in Fig. 2, except for the (11) beam.

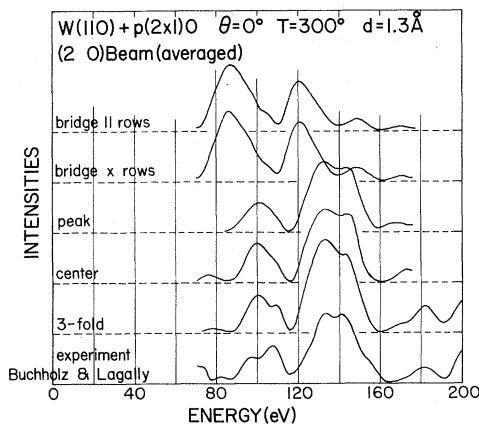


FIG. 4. Experimental (bottom curve) and calculated I - V curves for the (20) beam (averaged over domains) diffracted from the $W(110) + p(2 \times 1)O$ surface. The calculated curves apply to the five adsorption sites shown in Fig. 1 at the interlayer spacing 1.3 \AA . The experimental curve is taken from Ref. 7.

values are the same as those used in the clean $W(100)$ and $W(110)$ analyses.³ Time-saving features such as exploiting symmetry between reflected beams and calculating multiple-overlayer positions without recalculating the substrate diffraction make the computation cost substantially lower than if done by conventional dynamical LEED methods. Since tungsten is one of the strongest known electron scatterers, the success in obtaining numerical convergence by the layer-doubling method indicates the general applicability of this perturbation scheme.

We compare our results with data measured by Buchholz, Wang, and Lagally.⁷ In Figs. 2 and 3, we show the comparison between theory and experiment for the threefold adsorption site with different overlayer-substrate interlayer spacings. It is clear that the interlayer spacing of best fit is between 1.2 and 1.3 \AA (all calculated intensities have been averaged over the different domain orientations that the overlayer can have on the substrate). After considering five different beams we determine the optimal interlayer spacing to be $1.25 \pm 0.1 \text{ \AA}$. In Figs. 4 and 5, we show the comparison of various coordinated sites at the 1.3-\AA interlayer spacing. From Fig. 4, the comparison between theory and experiment for the (20) beam clearly rules out the two bridge positions. The peak, center, and threefold positions are compared in Fig. 5 for the $(\frac{1}{2} \frac{3}{2})$ beam and we find that the threefold site is favored over the other two locations. We have analyzed the level of agree-

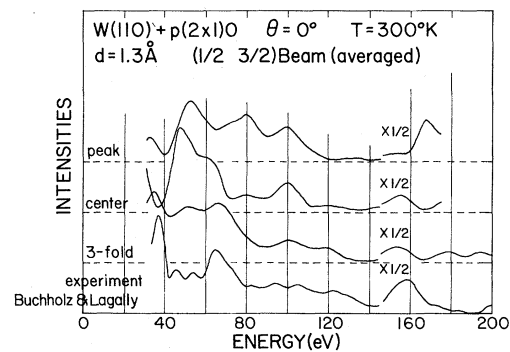


FIG. 5. The same as in Fig. 4, except for the $(\frac{1}{2} \frac{3}{2})$ beam with the threefold, center, and peak positions.

ment between theory and experiment for the different coordinated sites with several simple quantitative methods. The findings are shown in Figs. 6(a) and 6(b). By (i) counting the number of peaks that match between experiment and theory to within a window of 4 eV , by (ii) calculating the mean deviation between peak positions, by (iii) adding the total energy range in which experimental and theoretical I - V curves have slopes of opposite signs, and by (iv) visually rating the agreement between curves, we find that each scheme invariably indicates that the threefold adsorption site is preferred. A second (less likely) choice is the center site at 1.25 \AA , while the peak and two bridge positions can be completely ruled out as

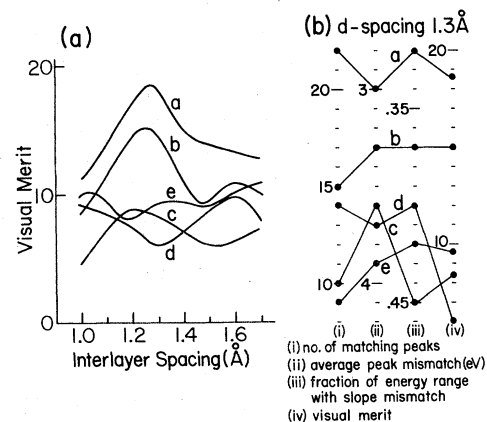


FIG. 6. Quantitative and visual methods for comparing the agreement between theory and experiment for the different binding sites. The five adsorption sites a - e are the same as those shown in Fig. 1. (a) Visual merit of the five sites versus different interlayer spacings. (b) Results of the various rating schemes for the five adsorption sites at interlayer spacing 1.3 \AA . The threefold site is preferred in each rating scheme.

possible binding sites.

From the determined threefold binding site at $1.25 \pm 0.1 \text{ \AA}$, the oxygen-tungsten chemisorption bond length is found to be $2.08 \pm 0.07 \text{ \AA}$, which is very close to the sum of covalent radii of oxygen and tungsten ($r_W + r_O = 2.12 \text{ \AA}$). The oxygen-tungsten bond length determined here is consistent with the trend observed for $c(2 \times 2)$ and $p(2 \times 2)$ oxygen chemisorption on nickel.^{8,9} Given an experimentally measured¹⁰ work function change of $\Delta\phi = 0.7 \text{ eV}$, we estimate the amount of charge transfer from tungsten to oxygen to be $q/e = 4.4\%$, where e is the electron charge.

*Work supported in part by the National Science Foundation Grant No. GH-40626.

¹M. A. Van Hove and S. Y. Tong, *J. Vac. Sci. Technol.* **12**, 230 (1975); J. B. Pendry, *Low-Energy Electron Diffraction Theory* (Academic, New York, 1974).

²See, for example, P. J. Estrup, *Phys. Today* **28**, No. 4, 33 (1975).

³M. A. Van Hove and S. Y. Tong, to be published.

⁴M. G. Lagally, J. C. Buchholz, and G.-C. Wang, *J. Vac. Sci. Technol.* **12**, 213 (1975).

⁵V. L. Moruzzi, A. R. Williams, and J. F. Janak, private communication. We are indebted to D. W. Jepsen for sending us the tungsten potentials.

⁶J. E. Demuth, private communication.

⁷J. C. Buchholz, G.-C. Wang, and M. G. Lagally, to be published; J. C. Buchholz, Ph.D. thesis, University of Wisconsin, 1974 (unpublished).

⁸S. Y. Tong, in *Progress in Surface Science*, edited by S. G. Davison (Pergamon, New York, 1975), Vol. 7, Part 2.

⁹P. M. Marcus, J. E. Demuth, and D. W. Jepsen, in *Proceedings of the Conference on Electron Diffraction Spectroscopy*, University of Warwick, Warwick, England, March 1975 (to be published).

¹⁰B. J. Hopkins and K. R. Pender, *Surf. Sci.* **5**, 155 (1966); J. C. Tracy and J. M. Blakely, *Surf. Sci.* **15**, 257 (1969).

Very Shallow Trapping State in Doped Germanium

M. Taniguchi, M. Hirano, and S. Narita

Department of Material Physics, Faculty of Engineering Science, Osaka University, Toyonaka, Osaka 560, Japan
(Received 16 July 1975)

Submillimeter photoconductivity in doped germanium has been studied with a lamellar grating spectrophotometer. The observed photoconductivity is ascribed to a shallow trapping state such as D^- or A^+ . However, our spectral peak energies and shapes are quite different from those previously reported by Gershenson, Gol'tsman, and Mel'nikov.

Submillimeter photoconductivity in doped-Ge and -Si crystals has been investigated by Gershenson and co-workers^{1,2} using backward-wave tubes (BWT). In the case of Ge, they observed photoconductive response peaks in the energy region of 1–2 meV depending on the kind of impurity used as dopant. They ascribed the responses to electrons (holes) bound to neutral donors (acceptors); that is, to D^- (A^+) states.

In the present experiment, we study the photoconductivities in Ge crystals doped with As, Sb, and Ga impurities using a Fourier transform spectrometer with a lamellar grating, and observe photoconductivity spectra having peaks near 3 meV and spreading widely from 1 to 7 meV. However, we do not observe any photoconductivity structure at the energy positions reported by Gershenson, Gol'tsman, and Mel'nikov.¹ The observed photoconductivity is confirmed to be due to a trapping center and it is in-

ferred that the D^- (A^+) state is also the most probable candidate for the center.

The spectrometer used was a Beckman LR-100 lamellar grating spectrophotometer designed to operate over the region $3\text{--}70 \text{ cm}^{-1}$. A combination of a low-pass filter and a cooled quartz filter was used to emphasize the required spectral range and to reduce the room-temperature background radiation above 250 cm^{-1} . The measured relative photoconductivity intensities were calibrated by measuring the spectral distribution of the light source (mercury vapor lamp) just at the front of the sample using a Unicam Golyay-cell detector. The accuracy of the wavelength scale of the spectrometer was verified by measuring the absorption spectra of a hexa-iodobenzene (C_6I_6) powder disk. The Ge specimens for the measurements were cut and shaped into about $4 \times 5 \times \sim 0.5 \text{ mm}^3$ pellets, mechanically polished, and CP-4 etched after being tapered to avoid in-